

Primary oscillatory instability in a rotating disk–cylinder system with aspect (height/radius) ratio varying from 0.1 to 1

A Yu Gelfgat

School of Mechanical Engineering, Faculty of Engineering, Tel-Aviv University,
Ramat Aviv, 69978 Tel-Aviv, Israel

E-mail: gelfgat@tau.ac.il

Received 4 March 2015

Accepted for publication 4 March 2015

Published 8 April 2015



Communicated by Edgar Knobloch

Abstract

Three-dimensional instability of axisymmetric flow in a rotating disk–cylinder configuration is studied numerically for the case of low cylinders with the height/radius aspect ratio varying between 1 and 0.1. A complete stability diagram for the transition from steady axisymmetric to oscillatory three-dimensional flow regime is reported. A good agreement with the experimental results is obtained. It is shown that the critical azimuthal wavenumber grows with the decrease of the aspect ratio, reaching the value of 19 at the aspect ratio 0.1. It is argued that the observed instability cannot be described as resulting from a boundary layer only. Other reasons that can destabilize the flow are discussed.

Keywords: confined swirling flow, hydrodynamic stability, Hopf bifurcation, rotor-stator cavity

(Some figures may appear in colour only in the online journal)

1. Introduction

Flow in a cylinder covered by a rotating disk has been one of most popular swirling flow models during several of the last few decades. Early studies (e.g. Escudier 1984, Lopez 1990, Lopez and Perry 1992) were mainly devoted to the phenomenon of vortex breakdown that the flow exhibits under certain conditions. Later, attention was focused on stability of the base axisymmetric flow (Gelfgat *et al* 1996, 2001), non-linear development of instabilities (Lopez *et al* 2001, Lopez 2006, Lopez *et al* 2006, 2008), stability control (Cui *et al* 2009, Tan

et al 2009) and the effects of some mechanical, thermal or electromagnetic flow complications (not cited here). The flow is governed by two dimensionless parameters that are usually chosen as Reynolds number Re , based on the disk radius and angular velocity, and height/radius aspect ratio γ . The early computational studies of flow stability (Gelfgat *et al* 1996, 2001) considered moderate aspect ratios $1 \leq \gamma \leq 3.5$ that corresponded to classical experiments of Escudier (1984). These results were verified numerically in several independent studies and later were validated experimentally by Sørensen *et al* (2006) so that their correctness seems to be proved. A similar cross-validation of numerical and experimental results was repeated later by Sørensen *et al* (2009) for higher cylinders with the aspect ratio reaching $\gamma = 6$.

Along with a large number of studies considering aspect ratios larger than unity, a group of authors examined the rotating disk–cylinder flow at small-aspect ratios, mainly at $\gamma = 0.25$ and 0.1 (see e.g. Cousin-Rittermand *et al* 1999a, 1999b, Gauthier *et al* 1999, Serre *et al* 2001, 2004, Serre and Pulicani 2001, Schouveiler *et al* 1998, 2001, Daube and Le Quéré 2002, Tuliszká-Sznitko *et al* 2002, Cross *et al* 2005; and references therein). Several authors emphasized the connection between the model and flows between rotating compressors and turbine disks (Serre *et al* 2001, 2004), calling the model ‘rotor-stator cavity’ or ‘rotor-stator system’. Also, for small-aspect-ratio configurations, the term ‘interdisk cavity’ is used (Pécheux and Foucault 2006) to distinguish them from ‘cylinder cavity’ configurations of moderate and large-aspect ratios. The main results of these studies are reviewed by Launder *et al* (2010). In the current study we are most interested in the results obtained for instability of the base axisymmetric flow in rotor-stator cavities, a brief examination of which shows that the numerical results (Serre *et al* 2001, 2004, Serre and Pulicani 2001, Daube and Le Quéré 2002) do not agree between themselves and also do not usually match corresponding experimental findings (Schouveiler *et al* 1998, 2001, Cross *et al* 2005), except in a recent study of Peres *et al* (2012). This disagreement motivated the present study, of which the main goal is the extension of our previous stability results to small-aspect ratio cylinders up to $\gamma = 0.1$.

In the following we examine three-dimensional instability of the axisymmetric base flow in the rotating disk–cylinder system for aspect ratios decreasing from 1 to 0.1. The linear stability analysis separates for different azimuthal Fourier modes so that we find the most critical circumferential periodicity (Fourier mode). In particular, we show that at $\gamma = 0.1$ the critical circumferential periodicity is $2\pi/19$, and we argue that this fact only can lead to certain numerical difficulties when a numerical grid is used. The present numerical results show parametric dependence of critical parameters on the aspect ratio gradually decreasing from 1 to 0.1. The results are successfully compared with the experiments (Schouveiler *et al* 1998, 2001, Cross *et al* 2005) and the recent direct numerical simulation of Peres *et al* (2012) at certain values of the aspect ratio considered in the cited studies.

Early studies of instabilities (see the review of Launder *et al* (2010) and references therein) considered the system at a very large Reynolds number in which the so-called Batchelor solution is valid and discovered two main types of instabilities: Type I instability related to the inflection point in the radial velocity profile and Type II instability arising in the rotating disk boundary layer. To gain some more insight in reasons causing flow destabilization, we present patterns of flows and the most unstable perturbations and perform some additional estimates and numerical experiments. This allows us to exclude the possibility of Type II instability. In the following we argue that instability sets in due to advection of azimuthal velocity along the cylinder side wall and then along the bottom toward the axis, where Type I instability can also develop.

Additionally, results of the linear stability analysis show that at small-aspect ratios perturbation modes with close azimuthal wavenumbers have also close marginal Reynolds

numbers. This indicates the possibility of multiple supercritical states, as was observed in the experiments of Schouveiler *et al* (1998).

2. Formulation of the problem and numerical method

We consider a flow of Newtonian incompressible liquid with density ρ and kinematic viscosity ν in a vertical cylindrical container of radius R and height H , of which the upper cover rotates around its axis with the angular velocity Ω . The flow is governed by the momentum and continuity equations that are rendered dimensionless using R , R^2/ν , ΩR and $\rho(\Omega R)^2$ as scales of length, time, velocity and pressure, respectively. The dimensionless equations and no-slip boundary conditions are defined in a cylinder $0 \leq z \leq \gamma$, $0 \leq r \leq 1$ and read

$$\frac{\partial \mathbf{v}}{\partial t} + (\mathbf{v} \cdot \nabla) \mathbf{v} = -\nabla p + \frac{1}{Re} \Delta \mathbf{v}, \quad (1)$$

$$\nabla \cdot \mathbf{v} = 0, \quad (2)$$

$$\mathbf{v}(r, z=0) = \mathbf{v}(r=1, z) = 0, \quad (3)$$

$$\psi(r, z=\gamma) = \psi_z(r, z=\gamma) = 0, \quad v_\theta(r, z=\gamma) = r. \quad (4)$$

Here, p is the pressure, $\mathbf{v} = \{v_r, v_\theta, v_z\}$ is the velocity, $\gamma = H/R$ is the aspect ratio of the cylinder and $Re = \Omega R^2/\nu$ is the Reynolds number. The problem is formulated in cylindrical coordinates so that the velocity and pressure fields are 2π -periodic with respect to the polar angle θ . In the following we assume that the base flow state $V = \{V_r(r, z), V_\theta(r, z), V_z(r, z)\}$ is steady and axisymmetric and examine its stability with respect to infinitesimally small three-dimensional disturbances, defined as $u = \{u_r(r, z), u_\theta(r, z), u_z(r, z)\} \exp(\lambda t + ik\theta)$. After the base flow is calculated, the linear stability problem reduces to an eigenvalue problem for the complex growth rate λ that separates for each integer azimuthal wavenumber k . For each aspect ratio γ we calculate marginal values of the Reynolds number $Re_m(k)$ at which the leading eigenvalue (i.e. eigenvalue with the largest real part) crosses the imaginary axis. The critical Reynolds number Re_{cr} is defined as the minimal $Re_m(k)$ over all values of k . Accordingly, the imaginary part of λ defines the marginal and circular critical frequency of disturbance oscillations in time, ω_m and ω_{cr} . More details on the problem formulation can be found in Lopez (1990), Lopez and Perry (1992) and Gelfgat *et al* (1992, 2001).

The problem is solved using finite volume discretization in space and the numerical approach described in Gelfgat (2007). In the above study the numerical method was already verified for arbitrary values of the aspect ratio and was validated against experimental results for $3.3 \leq \gamma \leq 5.5$ in Sørensen *et al* (2009). Therefore, we needed to examine the convergence mainly for the smallest value of the aspect ratio $\gamma = 0.1$, considered below. According to conclusions of Gelfgat (2007), a calculation of the critical Reynolds number needs at least 100 grid points in the shortest spatial direction, while results can be further improved using the Richardson extrapolation. Therefore, to ensure convergence we monitored marginal Reynolds numbers and frequencies for grid sizes varying from $N_z = 100$ to 200 and $N_r = N_z/\gamma$. A monotonic change of all values with grid refinement with an obvious tendency to convergence was observed. We concluded that for the numerical method used the discontinuity between the rotating disk and stationary side wall does not cause any numerical difficulties. Similarly to the calculations for $\gamma=1$ and 2.5 (Gelfgat 2007), we applied Richardson extrapolation to the results of the two finest grids. Thus, to calculate the stability diagrams, we performed two independent calculations on two grids with the number of axial points $N_z = 190$ and 200 ($N_r = N_z/\gamma$), followed by the Richardson extrapolation of the two

results. The results of calculations on the two grids differ only in the fifth decimal place. After Richardson extrapolation is done four first decimal places are considered as converged.

3. Results

The main stability results are shown in figures 1 and 2 for $0.2 \leq \gamma \leq 1$ and $0.1 \leq \gamma \leq 0.2$, respectively. Marginal Reynolds numbers Re_m calculated for different azimuthal wavenumbers k are shown in the frames (a). As mentioned above, at $Re = Re_m$ the largest real part of all the eigenvalues $\lambda(k)$ is zero, and the corresponding eigenvalue and eigenmode are called leading. The imaginary part of leading eigenvalue ω_m can be interpreted as a marginal value of the oscillation's circular frequency and is called marginal frequency. The marginal frequencies are shown in the frames (b) of figures 1 and 2. The disturbances are proportional to $\exp(ik\theta + i\omega_m t)$ so that they appear as waves travelling in the azimuthal direction with the phase angular velocity $\omega_m/2\pi k$. The disk is assumed to rotate with a positive angular frequency Ω in the (positive) counter-clockwise direction. Therefore, negative values of ω_m correspond to a wave travelling in the (negative) clockwise direction, opposite to the disk rotation. The parameter $a = R/2H$ used in several above-cited studies instead of the aspect ratio γ is shown as the upper horizontal axis of the frames (a).

Observing the critical values of the Reynolds numbers Re_{cr} , represented by the lower envelope of all curves in the frames (a), we see that at $\gamma = 1$ the instability sets in with the azimuthal number $k_{cr} = 2$ (figure 1(a)), as predicted in Gelfgat *et al* (2001) by another numerical technique and confirmed experimentally in Sørensen *et al* (2006). With the decrease of the aspect ratio the critical azimuthal wavenumber k_{cr} grows, becoming $k_{cr} = 3$ at $\gamma \approx 0.85$, $k_{cr} = 4$ at $\gamma \approx 0.5$, and $k_{cr} = 5$ at $\gamma \approx 0.4$ (figure 1(a)). With a further decrease of the aspect ratio the critical azimuthal wavenumber grows even more rapidly, reaching $k_{cr} = 10$ at $\gamma \approx 0.2$, and $k_{cr} = 19$ at $\gamma \approx 0.1$ (figure 2(a)). At these large values of k the marginal values of $Re_m(\gamma)$ are very close. The differences between marginal Reynolds numbers become so small that they can be distinguished by comparing the numbers but not by comparing the curves. To illustrate this, marginal Reynolds numbers and frequencies at $\gamma = 0.1$ and $15 \leq k \leq 25$ are reported in table 1. We observe that the critical Reynolds number at $k = 19$ is less than one percent smaller than Re_m at several neighbouring values of k . This means that selection of the azimuthal periodicity in supercritical flow regimes is dependent on the initial conditions so that multiplicity of the asymptotic oscillatory state at $Re > Re_{cr}$ can be expected. Experimental observations of Schouveiler *et al* (1998) confirm this conclusion. The curves of $\omega_m(\gamma)$ at different azimuthal wavenumbers are rather well separated (frames (b) in figures 1 and 2) so that the frequency value can serve as an indication of a certain azimuthal periodicity, as was done in experiments of Lopez *et al* (2008) and Sørensen *et al* (2006, 2009).

Another important conclusion that follows from the large azimuthal wavenumber instability observed at small-aspect ratios relates to requirements that any computational modelling of supercritical oscillatory flows should meet. To resolve the instability at $k_{cr} = 19$, the numerical method should account for at least 20 first Fourier harmonics ($0 \leq k \leq 19$). To account for the main non-linear effects the number of harmonics should be doubled. In the case of a numerical method using a grid in the circumferential direction, the number of grid nodes must be sufficient to resolve structures located within a sector defined by the angle of $2\pi/19$. Assuming a coarse resolution of 10 points per structure, we arrive at 190 azimuthal grid points. None of the previous calculations, carried out for $\gamma = 0.1$, met these accuracy requirements (see next section).

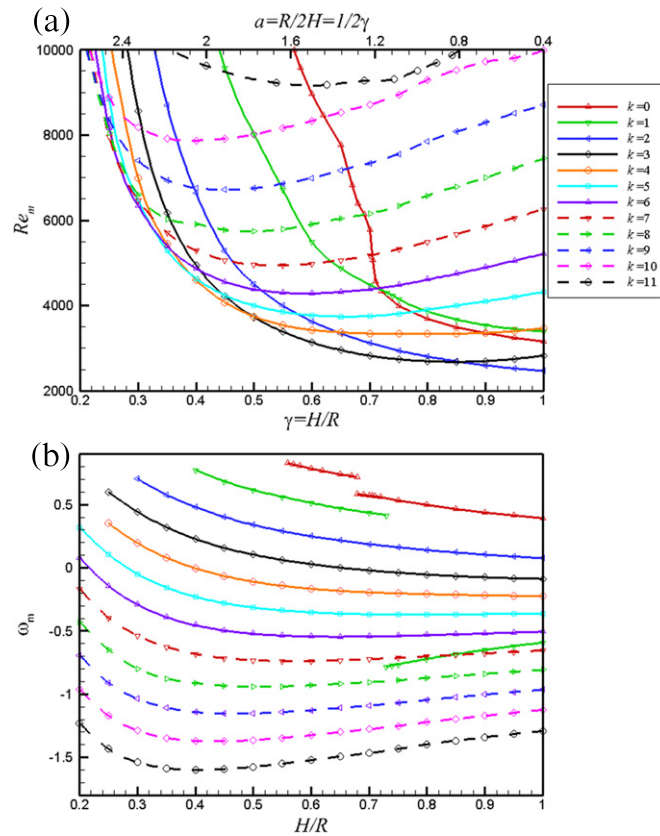


Figure 1. Marginal Reynolds numbers (a) and marginal oscillations frequencies (b) corresponding to different azimuthal wavenumbers k for an aspect ratio varying from 0.2 to 1.

Flow and leading perturbation patterns are illustrated in figures 3–5. The flow is shown by streamlines of the meridional flow (upper left frames) and isolines of the azimuthal velocity V_θ (upper right frames). Amplitude of the leading (or most unstable) perturbation $\mathbf{u}(r, z) = \{u_r(r, z), u_\theta(r, z), u_z(r, z)\}$ is a complex vector function, and we show real and imaginary parts together with the absolute value of all three components. Since the leading perturbation is an eigenvector of the linear stability problem, it is defined within multiplication by a constant. This means that values of maximal moduli reported in the figures can be used only by comparison of maxima of different perturbation components between themselves. Thus, we observe that perturbation of the azimuthal velocity is always larger than that of the two other velocity components. The absolute value of the perturbations represent distribution of the amplitude of flow oscillations in the meridional plane, while patterns of its real and imaginary parts correspond to two momentarily snapshots taken at a time interval of half an oscillation period. These two patterns are defined within multiplication by a real constant and a choice of their complex phase. Note that small structures of real and imaginary parts of perturbations appearing along the cylinder bottom in figures 4 and 5 require better spatial resolution than the base flow itself does. This is the main reason for applying fine grids, up to 2000×200 nodes, in the current study.

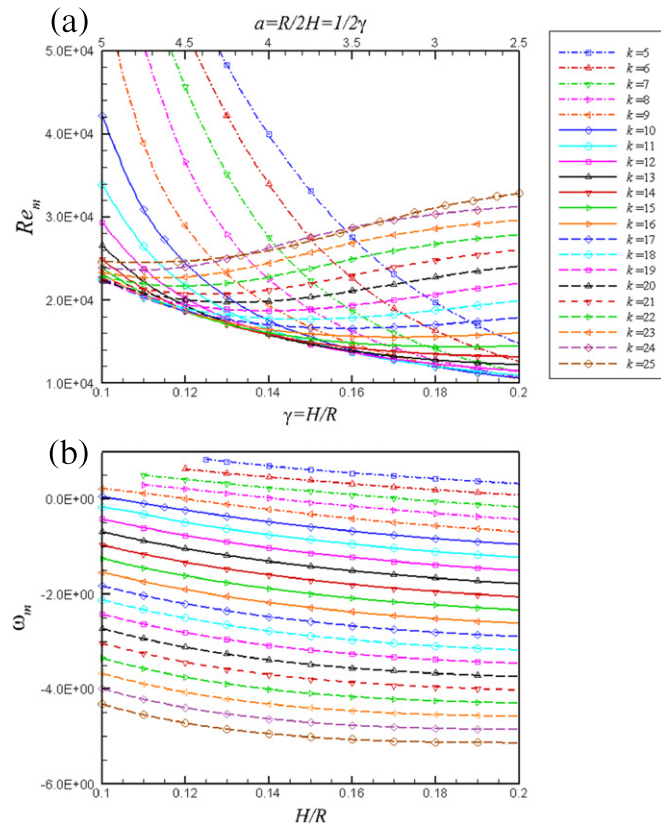


Figure 2. Marginal Reynolds numbers (a) and marginal oscillations frequencies (b) corresponding to different azimuthal wavenumbers k for an aspect ratio varying from 0.1 to 2.

Table 1. Marginal Reynolds numbers and frequencies at $\gamma=0.1$ and $15 \leq k \leq 25$.

k	Re_m	ω_m
15	23 866.	-1.2536
16	23 190.	-1.540 36
17	22 743.	-1.831 43
18	22 471.	-2.126 42
19	22 351.	-2.425 76
20	22 374.	-2.729 76
21	22 538.	-3.038 54
22	22 842.	-3.352 19
23	23 289.	-3.670 79
24	23 879.	-3.994 39
25	24 602.	-4.323 00

Patterns of the most unstable perturbations (figures 3–5) allow one to make several conclusions and some reasonable speculations about flow physics involved in the instability onset. First, we observe that the perturbations are most intensive near the stationary bottom of

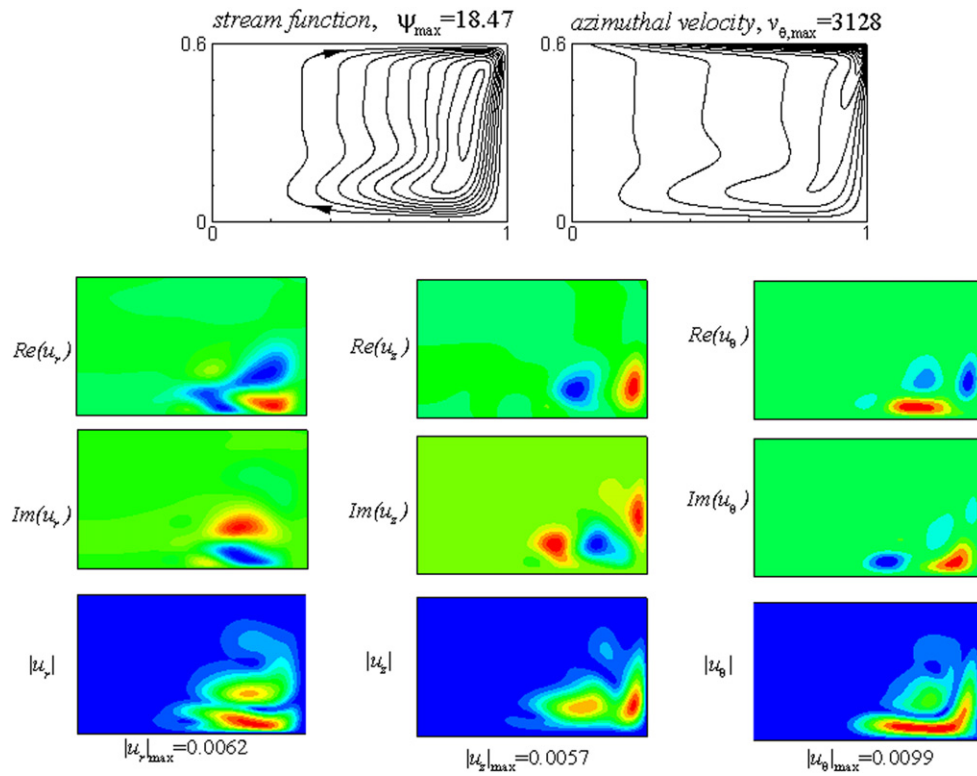


Figure 3. Base flow (upper frames) and patterns of the most unstable perturbation (dominant eigenmodes) $\mathbf{u} = \{u_r(r, z), u_\theta(r, z), u_z(r, z)\}$ at aspect ratio $\gamma = 0.6$.

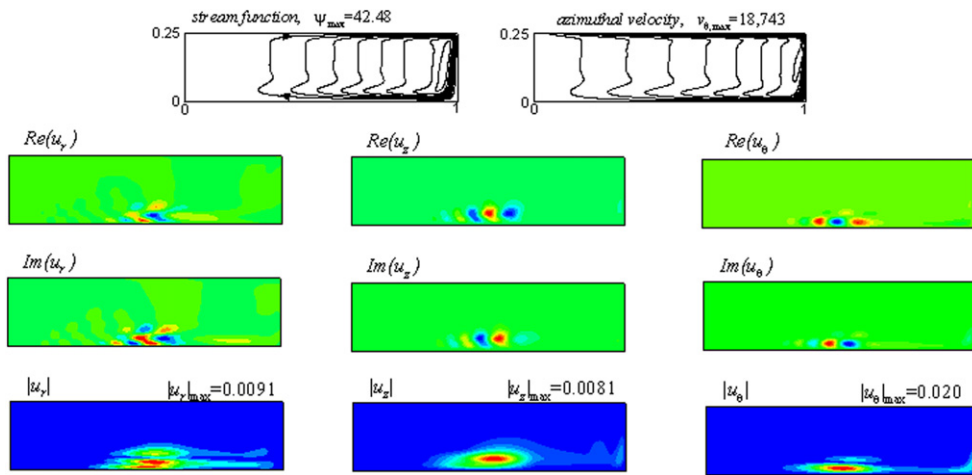


Figure 4. Base flow (upper frames) and patterns of the most unstable perturbation (dominant eigenmodes) $\mathbf{u} = \{u_r(r, z), u_\theta(r, z), u_z(r, z)\}$ at aspect ratio $\gamma = 0.25$.

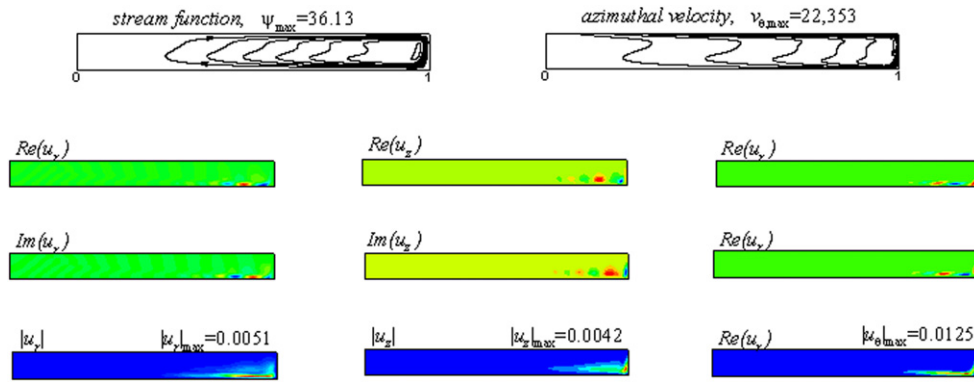
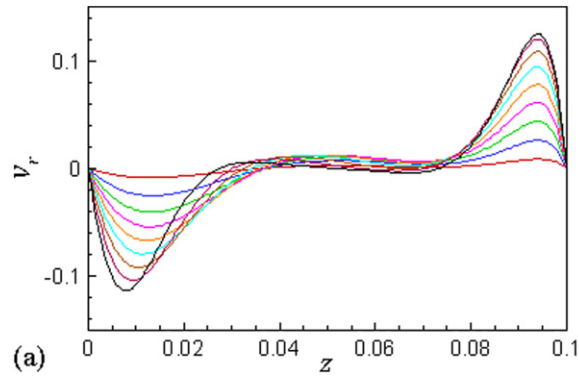
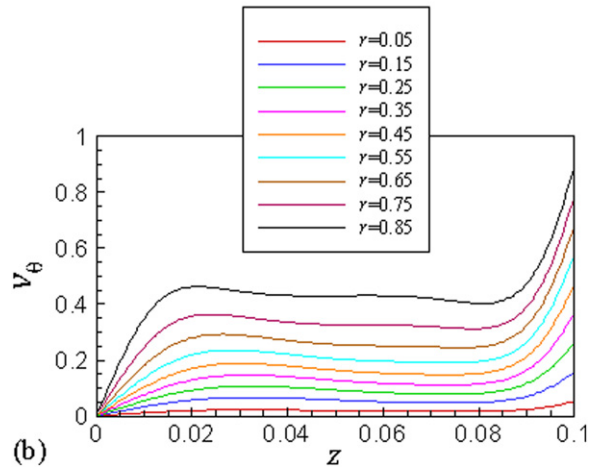


Figure 5. Base flow (upper frames) and patterns of the most unstable perturbation (dominant eigenmodes) $\mathbf{u} = \{u_r(r, z), u_\theta(r, z), u_z(r, z)\}$ at aspect ratio $\gamma=0.1$.



(a)



(b)

Figure 6. z -profiles of radial (a) and circumferential (b) velocities at different radii. $Re = 22\,350$; $\gamma = 0.1$.

the cylinder. These patterns show that the instability observed is not related to the Type II instability that sets in near the rotating disk. Localization of the most unstable perturbation near the stationary lower disk (figures 4 and 5) can possibly relate to Type I. In this case the radial velocity profile must have an inflection point inside the stationary disk boundary layer. Examination of the profiles (figure 6(a)) shows that, say at $\gamma=0.1$, the first inflection point appears at relatively small $z<0.02$ near the side wall, where $r>0.7$. This supports the presence of the Type I instability. On the other hand, the area, where inflection points are located inside the boundary layer, is characterized also by noticeably larger circumferential velocity (figure 6(b)). Profiles of the latter also have inflection points, but the points are outside the boundary layer. Moreover, the flow in this area is not plane-parallel so that the existence of the inflection point cannot be used as an indication of instability.

Instability of Type I rotating flow near the stationary disk was studied by Serre *et al* (2004), who found that it sets in as a travelling wave rotating in the direction opposite to the upper disk rotation. This qualitatively agrees with the present negative values of ω_m . Furthermore, the instabilities were predicted to set in at local Reynolds number $Re_\delta = 47.5$, where $Re_\delta = r^*\sqrt{\Omega/\nu}$, and r^* is the local distance to the axis. Using a rough estimation $r^* = 0.5R$ and $Re_{cr} \approx 2 \cdot 10^4$ (figure 2), we estimate $Re_\delta \approx 0.5\sqrt{Re} \approx 70$, which also fits the above prediction. We could not find, however, how the theoretical results of Serre *et al* (2004) can predict a large critical azimuthal wavenumber. Also, the above arguments do not relate to the perturbation patterns shown in figure 3 for $\gamma = 0.6$. In this case we observe also a large perturbation amplitude near the cylinder wall. A closer look on the disturbances moduli shown in figures 4 and 5 also reveals a possible effect of the lateral wall on the flow instability.

Looking for another possible explanation of instability we notice again that the most intensive disturbances are located near the stationary bottom, where the main meridional circulation is directed from the cylinder wall toward the axis. This is reminiscent of a well-known instability mechanism in which azimuthal velocity perturbation is advected toward the rotation axis and increases owing to conservation of the rotational momentum. Such instability takes place in inviscid rotating flows when the Rayleigh criterion $\frac{\partial}{\partial r}(rV_\theta)^2$ becomes negative. A more comprehensive criterion for inviscid instability of a columnar vortex was developed by Leibovich and Stewartson (1983). According to their result, the sufficient condition for instability is existence of a point where the expression $V_\theta \frac{\partial}{\partial r} \left(\frac{V_\theta}{r} \right) \left[\frac{\partial}{\partial r} \left(\frac{V_\theta}{r} \right) \frac{\partial(rV_\theta)}{\partial r} + \left(\frac{\partial V_\theta}{\partial r} \right)^2 \right]$ is negative. Both criteria are plotted in figures 7 and 8 and look similar. We observe that they are positive along most of the stationary bottom and become strongly negative along the stationary cylinder wall, where the azimuthal velocity steeply decreases. The largest negative magnitudes of both criteria are located near the upper corner where the azimuthal velocity is discontinuous; however, no strong disturbances are observed there. Slightly negative values of both criteria persist in the lower corner of the cylinder, where non-negligible perturbation amplitudes were observed. As is seen from figures 7 and 8, the relative negative magnitude of both criteria grows with the decrease of the aspect ratio. Since viscosity effects are necessarily strong near the corners and changes of the meridional velocities are steeper than that of the rotational one, neither of the two criteria is applicable there.

We applied also the approach of Gelfgat (2011) in which different terms of the linear stability problem are cancelled one by one, while observing the cancellation of which leads to flow stabilization. Here, ‘flow stabilization’ means a change of sign of the leading eigenvalue from positive to negative. This exercise shows that cancellation of the terms $V_r \frac{\partial u_r}{\partial r}$, $V_r \frac{\partial u_\theta}{\partial r}$ and

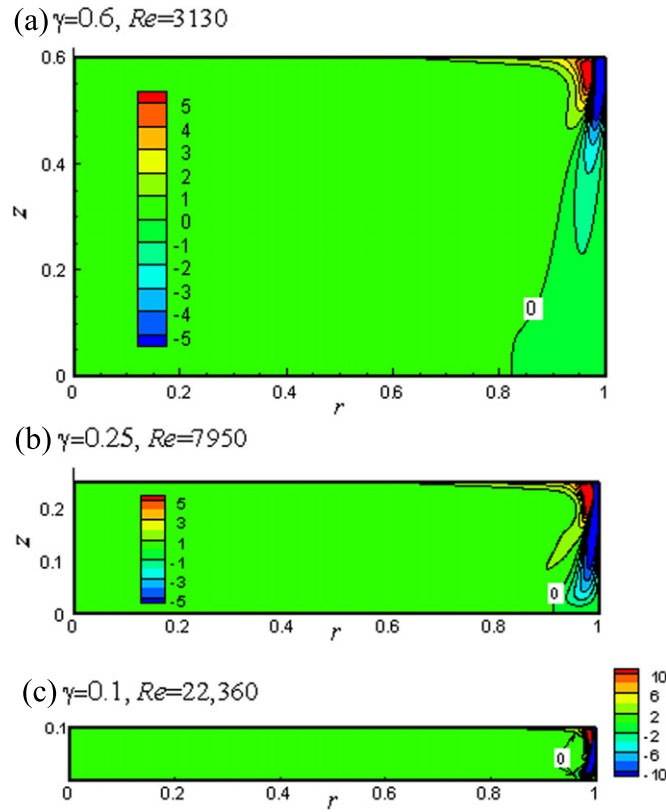


Figure 7. Isolines of Rayleigh stability criterion $\frac{\partial}{\partial r}(rV_0)^2$.

$V_r \frac{\partial u_c}{\partial r}$ does not yield any stabilization, which causes additional doubts about instability of the boundary layer in which the radial base velocity is dominant. At the same time it was observed that the strongest stabilization is achieved when the term $V_z \frac{\partial w}{\partial z}$ is excluded. Note that V_z is large near the side wall but is very small near the bottom stationary disk. Cancellation of several other terms (including those corresponding to perturbations of the centrifugal and Coriolis forces) provided weaker stabilization. Taking into account the perturbation patterns (figures 3–5) we can speculate that a disturbance of the azimuthal velocity is advected along the vertical wall toward the bottom, where the meridional flow changes its direction and drives the perturbations toward the axis. Along this motion the perturbation of the azimuthal velocity necessarily grows owing to conservation of the rotational momentum, thus leading to observation of strongly perturbed flow near the stationary disk, which may relate to the instability of Type I. This growth affects the centrifugal and Coriolis forces. The centrifugal force acts against the flow directed toward the axis, which can be a source of flow oscillations. The Coriolis force drives the perturbations in the azimuthal direction, which can lead to the appearance of the azimuthal travelling wave.

Observing that the relative height of the cylinder defines the critical azimuthal wave-number, we can connect them by estimating circumferential length of the most critical perturbation near the side wall. Measured in units of the height it is $(2\pi R/k_{cr} H) = 2\pi/k_{cr} \gamma$. Calculation of the value of $k_{cr} \gamma$ from the results of figures 1 and 2 shows that this product

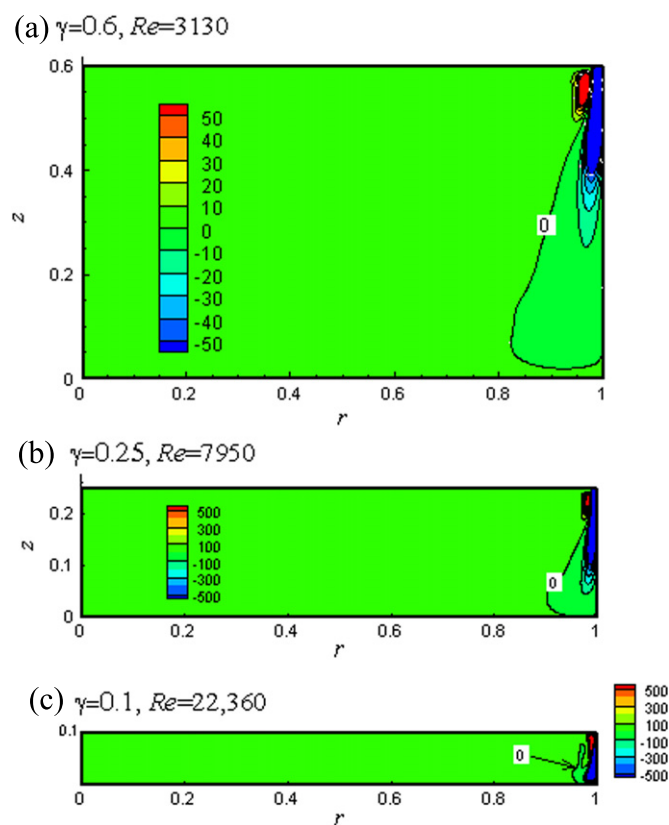


Figure 8. Isolines of Leibovich–Stewartson stability criterion $V_{\psi}^2 \frac{\partial}{\partial r} \left(\frac{V_{\psi}}{r} \right) \left[\frac{\partial}{\partial r} \left(\frac{V_{\psi}}{r} \right) \frac{\partial(rV_{\psi})}{\partial r} + \left(\frac{\partial V_{\psi}}{\partial r} \right)^2 \right]$.

varies from 0.526 to 0.555 for γ , varying from 0.1 to 0.3. Since k_{cr} attains only integer values the latter product is almost a constant, and we conclude that in low enough cylinders ($\gamma < 0.3$) the circumferential length of the most unstable perturbation near the side wall is approximately $(2\pi/0.54)H$. This almost constant value indicates again the importance of perturbation growth near the cylindrical boundary.

Note that similar growth of perturbations along the vertical wall and the stationary disk was observed by Poncet *et al* (2009) and Lopez *et al* (2009) for slightly different configurations. Thus, Poncet *et al* (2009) observed a similar instability mechanism for the appearance of axisymmetric circular waves ($k_{cr} = 0$) in the rotor-stator cavity with an inner hub for $\gamma=0.114$. Lopez *et al* (2009) considered the same configuration as here, but with the side wall rotating together with the disk. For $\gamma=0.2$, they observed a noticeably larger critical azimuthal wavenumber $k_{cr} = 32$ but with a similar instability evolution.

4. Comparison with experiments and previous calculations

The transition from the steady to oscillatory flow regime was studied experimentally by Schouveiler *et al* (1998) and Cros *et al* (2005) for $\gamma = 0.114$ and by Schouveiler *et al* (2001) for

various aspect ratios, most of which were smaller than 0.1. The measured critical Reynolds numbers are 25 000 for $\gamma = 0.1$ and 20 500 for $\gamma = 0.114$. The frequency of the oscillating supercritical regime was reported only by Cros *et al* (2005) as $\omega = 2.1$ for $\gamma = 0.114$. The results of present calculations yield at $\gamma = 0.1$: $Re_{cr} = 22\,350$, $\omega_{cr} = 2.426$, $k_{cr} = 19$; and for $\gamma = 0.114$: $Re_{cr} = 19\,580$, $\omega_{cr} = 2.108$, $k_{cr} = 17$. Thus, our numerical results are in a good agreement with the experimental measurements. The experimental critical values of the Reynolds number are slightly above the numerical ones, as one would expect for a supercritical bifurcation. Additionally, we recall multiple three-dimensional states observed by Schouveiler *et al* (1998) at slightly supercritical Reynolds numbers. This confirms qualitatively our stability results that show close marginal Reynolds numbers at close values of the azimuthal wavenumber (table 1).

A comparison with the previously published numerical results appears to be only partially successful. Thus, the result reported for $\gamma = 0.25$ by Serre *et al* (2001) and Serre and Pulicani (2001) is $Re_{cr} = 16\,000$, $\omega_{cr} \approx 0.9$. The critical azimuthal wavenumber was not reported. The present result is $Re_{cr} = 7960$, $\omega_{cr} = 0.395$, $k_{cr} = 7$. The cited calculations used only 48 grid nodes in the azimuthal direction, which left only 6–7 grid nodes per azimuthal period at $k = 7$. This is clearly insufficient and can be the main reason for the disagreement. Earlier calculations made for $\gamma = 0.1$ reported $Re_{cr} = 35\,000$, $\omega_{cr} \approx 1.0$ (Serre and Pulicani 2001) and $Re_{cr} = 12\,000$, $\omega_{cr} \approx 1.5$ (Serre *et al* 2004). These critical Reynolds numbers are above and below the one reported here: $Re_{cr} = 22\,350$ (see above paragraph). Both calculations used 48 grid points in the azimuthal direction, which does not seem sufficient for $\gamma = 0.25$. Obviously, with such an insufficient number of points it was impossible to resolve the instability at $k_{cr} = 19$. Later computation by Peres *et al* (2012) applied 128 collocation points in the azimuthal direction at $\gamma = 0.114$ and arrived at $Re_{cr} = 20\,900$, $\omega_{cr} \approx 2.09$ and $k_{cr} = 17$, which agrees well with the present result. It is noticeable that 128 collocation points, which yield approximately 7.5 points per azimuthal structure, were sufficient for obtaining rather accurate critical parameters. Also, Poncet *et al* (2009) reported $k_{cr} = 17$ for a rotor-stator cavity with a hub and with $\gamma = 0.114$, using only 100 points in the azimuthal direction.

5. Conclusions

Study of three-dimensional instability of flow in a rotating disk–cylinder system is extended to low-aspect ratio containers, up to the height/radius ratio 0.1. The main stability results are reported as dependencies of the marginal Reynolds numbers and marginal frequencies on the aspect ratio and the azimuthal wavenumber k . It is found that the critical azimuthal wavenumber grows with the decrease of the aspect ratio γ so that $k_{cr} = 10$ at $\gamma \approx 0.2$, and $k_{cr} = 19$ at $\gamma \approx 0.1$. At small-aspect ratios we observe close marginal values of the Reynolds number corresponding to k close to k_{cr} , which can lead to multiplicity of stable oscillatory supercritical states, as was observed by Schouveiler *et al* (1998). The azimuthal modes can be distinguished, in particular, by their oscillation frequencies, of which the marginal values remain noticeably different at different k .

A good agreement with the experimental measurements of instability at $\gamma = 0.1$ and 0.114 are reported, which, together with the results of Sørensen *et al* (2006, 2009), completes the experimental validation of our present and previous stability results. A successful comparison with numerical results is obtained only with the recently published study of Peres *et al* (2012). Earlier results differ noticeably from the present ones. We argue that the disagreement

follows mainly from insufficient numerical resolution in the azimuthal direction so that the previous studies could not resolve instabilities at $k \geq 7$.

After several estimations and numerical experiments we argued that the observed instability cannot be described solely as instability of one of the boundary layers attached to either a rotating or stationary disk, e.g. Types I and II instabilities (Lauder *et al* 2010). Patterns of the most unstable perturbations show that the instability sets in the descending flow along the side wall and then grows additionally when advected along the stationary cylinder bottom toward the axis, where it increases due to conservation of the angular momentum and then affects the radial and circumferential fluid motion. This disturbance's growth along the stationary disk can relate to Type I instability.

We found also that in cylinders with $\gamma < 0.3$, the circumferential length of the most dominant perturbation structure near the side wall remains almost constant and can be estimated as $\approx 3.7\pi H$.

Acknowledgments

This study was supported by the Israel Science Foundation (Grant 426/12) and in part by the Wolfson Family Charitable Trust pr/ylr/18921 & 18837. The author is thankful to L Tuckerman for his useful and encouraging discussions.

References

- Cousin-Rittermard N, Daube O and Le Quéré P 1999a Description of the boundary layers of steady flows between coaxial disks in rotor-stator configuration *C. R. Acad. Sci. Paris Sér. IIB* **327** 215–20
- Cousin-Rittermard N, Daube O and Le Quéré P 1999b Structure of steady flows between coaxial disks in rotor-stator configuration *C. R. Acad. Sci. Paris Sér. IIB* **327** 221–6
- Cros A, Floriani E, Le Gal P and Lima R 2005 Transition to turbulence of the Batchelor flow in a rotor/stator device *Eur. J. Mech.* **24** 409–42
- Cui Y D, Lopez J M, Lim T T and Marques F 2009 Harmonically forced enclosed swirling flow *Phys. Fluids* **21** 034105
- Daube O and Le Quéré P 2002 Numerical investigation of the first bifurcation for the flow in a rotor-stator cavity of radial aspect ratio 10 *Comput. Fluids* **31** 481–94
- Escudier M P 1984 Observations of the flow produced in a cylindrical container by a rotating endwall *Exp. Fluids* **2** 189–96
- Gauthier G, Gondret P and Rabaud M 1999 Axisymmetric propagating vortices in the flow between a stationary and a rotating disk enclosed by a cylinder *J. Fluid Mech.* **386** 105–26
- Gelfgat A Y, Bar-Yoseph P Z and Solan A 1996 Stability of confined swirling flow with and without vortex breakdown *J. Fluid Mech.* **311** 1–36
- Gelfgat A Y, Bar-Yoseph P Z and Solan A 2001 Three-dimensional instability of axisymmetric flow in rotating lid-cylinder enclosure *J. Fluid Mech.* **438** 363–77
- Gelfgat A Y 2007 Three-dimensional instability of axisymmetric flows: solution of benchmark problems by a low-order finite volume method *Int. J. Numer. Meths. Fluids* **54** 269–94
- Gelfgat A Y 2011 Destabilization of convection by weak rotation *J. Fluid Mech.* **685** 377–412
- Lauder B, Poncet S and Serre E 2010 Laminar, transitional and turbulent flows in rotor-stator cavities *Ann. Rev. Fluid Mech.* **42** 229–48
- Leibovich S and Stewartson K 1983 A sufficient condition for the instability of columnar vortices *J. Fluid Mech.* **126** 335–56
- Lopez J M 1990 Axisymmetric vortex breakdown: 1. Confined swirling flow *J. Fluid Mech.* **221** 533–52
- Lopez J M and Perry A D 1992 Axisymmetric vortex breakdown: 3. Onset of periodic flow and chaotic advection *J. Fluid Mech.* **234** 449–71
- Lopez J M, Marques F and Sanchez F 2001 Oscillatory modes in an enclosed swirling flow *J. Fluid Mech.* **439** 109–29

- Lopez J M 2006 Rotating and modulated rotating waves in transitions of an enclosed swirling flow *J. Fluid Mech.* **553** 323–46
- Lopez J M, Cui Y D and Lim T T 2006 Experimental and numerical investigation of the competition between axisymmetric time-periodic modes in an enclosed swirling flow *Phys. Fluids* **18** 104106
- Lopez J M, Cui Y D, Marques F and Lim T T 2008 Quenching of vortex breakdown oscillations via harmonic modulation *J. Fluid Mech.* **599** 441–64
- Lopez J M, Marques F, Rubio A N and Avila N 2009 Cross flow instability of finite Bödewadt flows: transient and spiral waves *Phys. Fluids* **21** 114107
- Lopez J M 2012 Three-dimensional swirling flows in a tall cylinder driven by a rotating endwall *Phys. Fluids* **24** 014101
- Pécheux J and Foucault E 2006 Axisymmetric instabilities between coaxial rotating disks *J. Fluid Mech.* **563** 293–318
- Peres N, Poncet S and Serre E 2012 A 3D pseudospectral method for cylindrical coordinates. Application to the simulations of rotating cavity flows *J. Comput. Phys.* **231** 6290–305
- Poncet S, Serre E and Le Gal P 2009 Revisiting the two first instabilities of the flow in an annular rotor-stator cavity *Phys. Fluids* **21** 064106
- Schouveiler L, Le Gal P and Chauve M P 1998 Stability of a traveling roll system in a rotating disk flow *Phys. Fluids* **10** 2695–7
- Schouveiler L, Le Gal P and Chauve M P 2001 Instabilities of the flow between a rotating and a stationary disk *J. Fluid Mech.* **443** 329–50
- Serre E, Crespo del Arco E and Bontoux P 2001 Annular and spiral patterns in flows between rotating and stationary discs *J. Fluid Mech.* **434** 65–100
- Serre E and Pulicani J P 2001 A three-dimensional pseudo-spectral method for rotating flows in a cylinder *Comput. Fluids* **30** 491–519
- Serre E, Tuluszka-Sznitko E and Bontoux P 2004 Coupled numerical and theoretical study of the flow transition between a rotating and stationary disk *Phys. Fluids* **16** 688–706
- Sørensen J N, Naumov I V and Mikkelsen R F 2006 Experimental investigation in three-dimensional flow instabilities in a rotating lid-driven cavity *Exp. Fluids* **41** 425–40
- Sørensen J N, Gelfgat A Y, Naumov I V and Mikkelsen R F 2009 Experimental and numerical results on three-dimensional instabilities in a rotating disk–tall cylinder flow *Phys. Fluids* **21** 054102
- Tan B T, Liow K Y S, Mununga L, Thompson M C and Hourigan K 2009 Simulation of the control of vortex breakdown in a closed cylinder using a small rotating disk *Phys. Fluids* **21** 024104
- Tuluszka-Sznitko E, Bontoux P and Serre E 2002 On the nature of the boundary layers instabilities in a flow between a rotating and a stationary disk *C. R. Mechanue* **330** 91–9